Thermochimica Acta, 186 (1991) 43–52
Elsevier Science Publishers B.V., Amsterdam

Thermal studies on 1-hydroxypyridine-2-thione complexes of VO(IV), Cr(III), Mn(II), Fe(III), Co(II), Ni(II), Cu(II) and Zn(II)

F.J. Higes-Rolando, A. Pérez-Florindo[1] and C. Valenzuela-Calahorro
Departamento de Química Inorgánica, Universidad de Extremadura, Badajoz (Spain)

(Received 27 November 1990)

Abstract

The thermal behaviour of the complexes of 1-hydroxypyridine-2-thione with the cations VO(IV), Cr(III), Mn(II), Fe(III), Co(II), Ni(II), Cu(II) and Zn(II) have been studied using thermogravimetric (TG) and differential scanning calorimetric (DSC) methods. Intermediate and end-products from the decompositions in air have been investigated by X-ray powder diffractometry and IR spectroscopy. Decomposition processes have been proposed for these complexes.

INTRODUCTION

Since the preparation of 1-hydroxypyridine-2-thione (A) or its tautomer 2-pyridinethiol-1-oxide (B) (abbreviated PTOH), (see Fig. 1) with the former considered to be the dominant form [1], a variety of metal ion complexes have been isolated and characterised [2–9]. The formation of metal ion complexes occurs with the conjugate base of PTOH, with both the *N*-oxide oxygen and the sulphur atom serving as donors. Some of these complexes show biological activity and have been used as anti-fungal [10–12] and anti-bacterial [13–15] agents. Furthermore, PTOH has been used as a reagent in several titrimetric, spectrophotometric and gravimetric determinations of metallic ions [16–21].

Fig. 1.

[1] Author to whom correspondence should be addressed.

0040-6031/91/$03.50

A thermal stability study of several rare earth complexes of PTOH has been carried out by West and Frank [6]. In most cases, two different decomposition steps were identified in the anhydrous complexes. The initial step involves dissociation of one ligand from the metal. The second step involves breaking of the N–O and S–M bonds and release of one mole of pyridine-2-thione.

This paper reports the thermal behaviour of the complexes formed by PTOH and the cations VO(IV), Cr(III), Mn(II), Fe(III), Co(II), Ni(II), Cu(II) and Zn(II), using TG–DTG and DSC techniques. Decomposition processes were followed by X-ray powder diffractometry and IR spectroscopy.

EXPERIMENTAL

Reagents

The sodium salt of 1-hydroxypyridine-2-thione (NaPTO) was purchased from Sigma Chem. Comp. Ltd. and was used as received. Vanadium(III) chloride was used to obtain the oxovanadium(IV) complex. For the rest of the complexes, the corresponding nitrates (Merck R.A.) were used.

Preparation of compounds

All the complexes were prepared in the following general way: 25 ml of a 0.1 M solution of NaPTO were added with stirring to 25 ml of a 0.1 M solution of the appropriate metallic salt. The precipitate obtained was collected by filtration and washed with water, ethanol and ether. The complexes were dried in a desiccator over calcium chloride.

Apparatus

Carbon, hydrogen and nitrogen were analysed using a Perkin–Elmer 240-C elemental analyser. In the complexes of manganese(II), iron(III), copper(II) and zinc(II), the concentration of the metal ion was determined using a Perkin–Elmer 370 atomic absorption spectrophotometer. For the other complexes, colorimetric methods were used [22].

Infrared spectra were recorded as KBr discs using a Perkin–Elmer 1720 FTIR spectrophotometer in the 4000–400 cm^{-1} region and as polyethylene plates on a Beckman 42-50 spectrophotometer in the 600–200 cm^{-1} range.

X-Ray powder diffraction patterns were obtained with a Philips PW 1700 diffractometer using Cu Kα radiation.

Thermal studies were carried out on a Mettler MTA 3000 system provided with a Mettler TG 50 thermobalance and a Mettler DSC-20 differential scanning calorimeter. The TG curves were obtained in a dynamic air

atmosphere (flow rate, 100 ml min^{-1}) using samples varying in weight from 8.864 to 11.426 mg and at a heating rate of 10 °C min^{-1}. The DSC curves were recorded at a heating rate of 10 °C min^{-1} in a temperature range of 40–600 °C using sample weights varying from 1.827 to 2.439 mg.

RESULTS AND DISCUSSION

The solid complexes isolated have a stoichiometry of 1:2 for VO(IV), Mn(II), Co(II), Ni(II), Cu(II) and Zn(II), and 1:3 for Cr(III) and Fe(III) (Table 1).

The analytical data suggest that the manganese(II) complex is precipitated in the hydrated form.

TG–DTG and DSC curves for the complexes are given in Figs. 2 and 3. The thermoanalytical data are summarised in Table 2.

VO(PTO)$_2$

The TG curve for the oxovanadium(IV) complex shows that this solid is stable up to 148 °C, above which point thermal decomposition begins. The first stage of the decomposition continues up to 165 °C. The mass loss associated with this process is in good agreement with the removal of a pyridine *N*-oxide fragment (obs., 28.9%; calc., 29.5%). This effect is marked on the DSC curve by an exothermic peak at 160 °C. Between 165 and

TABLE 1

Analytical data and colour of the isolated complexes

Complex	Colour	Analysis found (%)			
		C	H	N	M
$VO(PTO)_2$	Violet	37.92	2.46	8.78	15.31
		(37.62)	(2.53)	(8.78)	(15.96)
$Cr(PTO)_3$	Green	41.74	2.85	9.76	11.81
		(41.85)	(2.81)	(9.76)	(12.08)
$Mn(PTO)_2 \cdot H_2O$	Yellow–green	36.66	2.87	8.45	16.98
		(36.93)	(2.81)	(8.61)	(16.89)
$Fe(PTO)_3$	Black	41.59	2.70	9.70	12.67
		(41.48)	(2.78)	(9.67)	(12.86)
$Co(PTO)_2$	Yellow–ochre	38.52	2.54	8.94	19.15
		(38.59)	(2.59)	(9.00)	(18.93)
$Ni(PTO)_2$	Brown	38.28	2.43	9.05	18.97
		(38.62)	(2.59)	(9.01)	(18.88)
$Cu(PTO)_2$	Pale green	37.65	2.49	8.65	19.87
		(38.03)	(2.55)	(8.87)	(20.12)
$Zn(PTO)_2$	White	37.91	2.58	8.45	20.62
		(37.81)	(2.54)	(8.81)	(20.58)

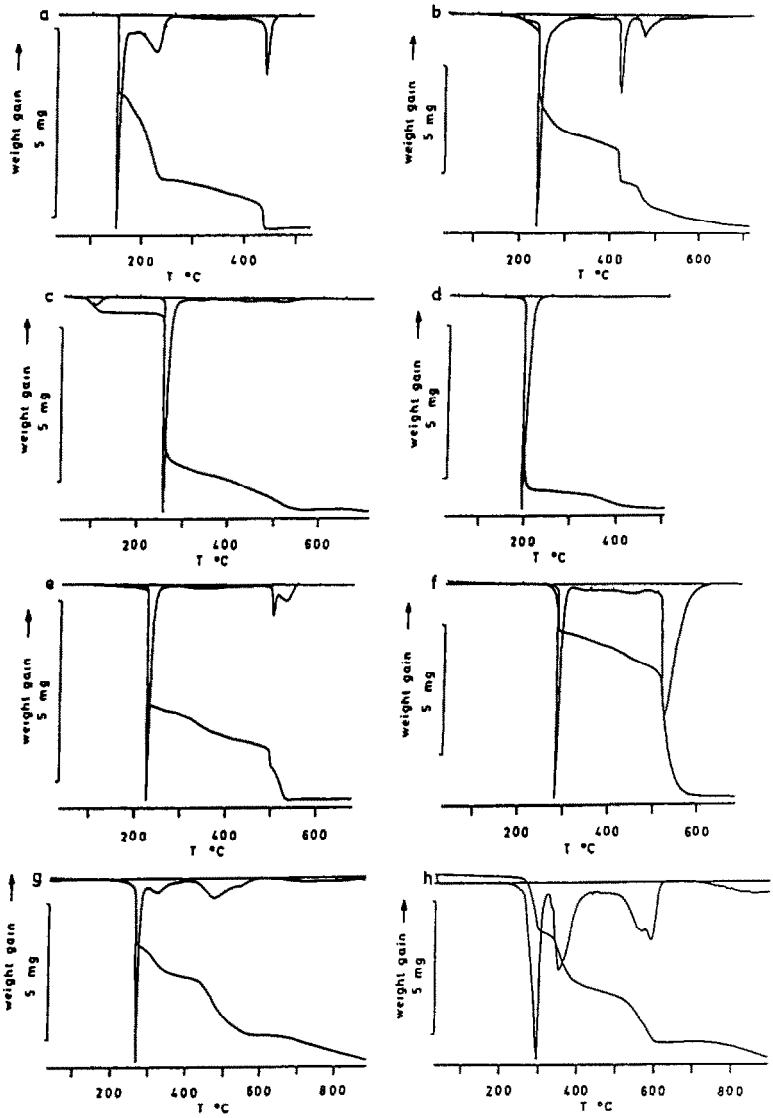

Fig. 2. TG curves for: (a) $VO(PTO)_2$; (b) $Cr(PTO)_3$; (c) $Mn(PTO)_2 \cdot H_2O$; (d) $Fe(PTO)_3$; (e) $Co(PTO)_2$; (f) $Ni(PTO)_2$; (g) $Cu(PTO)_2$; and (h) $Zn(PTO)_2$.

258 °C, a second pyridine *N*-oxide fragment is expelled (obs., 30.1%). This stage can be detected as a broad exothermic effect on the DSC curve at 245 °C. From 258 to about 420 °C, a slow weight loss occurs, accompanied by two weak exothermic peaks at 309 and 327 °C. This is immediately followed by a sudden decomposition situated at 438 °C on the DTG curve. Above 450 °C, the residue fails to undergo any appreciable mass variation. The X-ray pattern and IR spectrum reveal that the residue is V_2O_5 (exp., 28.2%; calc., 28.5%). The last stages of the complex pyrolysis and the

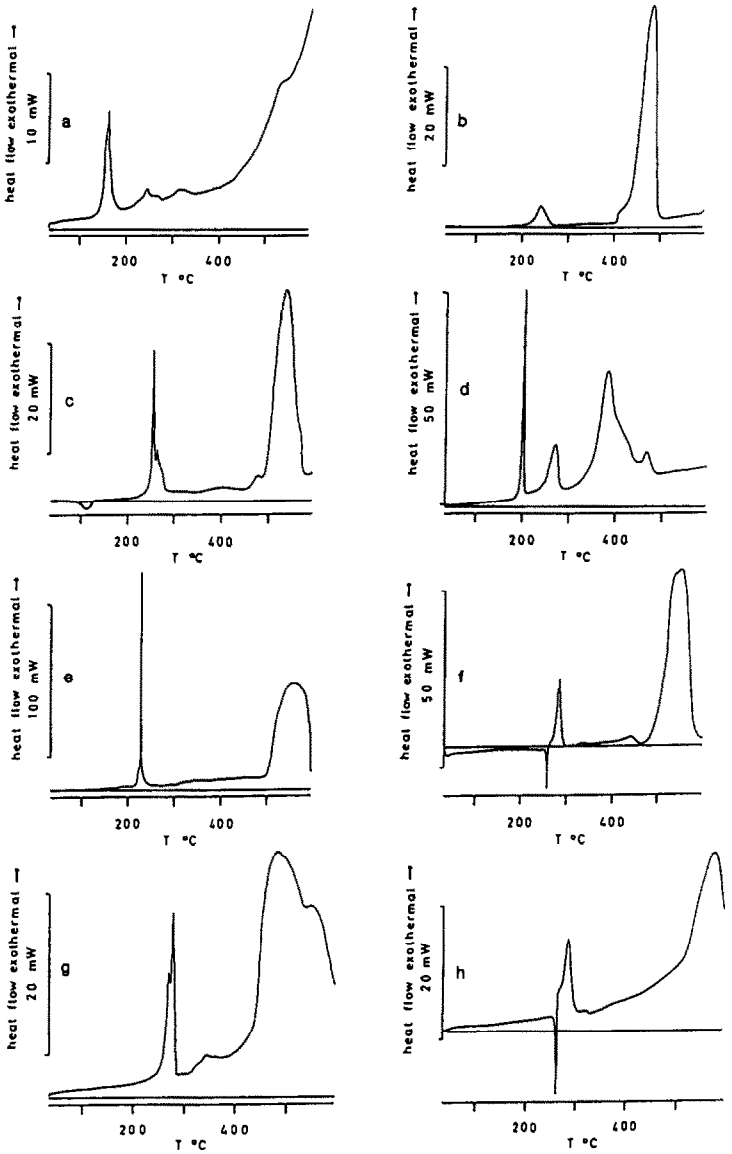

Fig. 3. DSC curves for: (a) $VO(PTO)_2$; (b) $Cr(PTO)_3$; (c) $Mn(PTO)_2 \cdot H_2O$; (d) $Fe(PTO)_3$; (e) $Co(PTO)_2$; (f) $Ni(PTO)_2$; (g) $Cu(PTO)_2$; and (h) $Zn(PTO)_2$.

oxidation process to V(V) give rise to the strong exothermic effect which begins at 355 °C. The maxima of this effect could be out of the instrumental limit.

$Cr(PTO)_3$

From the TG curve, it is observed that the mass change begins at 175 °C. There is, however, a major mass loss in the range 230–320 °C, associated

TABLE 2

Thermoanalytical data

Complex	Temp. range in TG (°C)	Peak temp. in DTG (°C)	Loss from TG (%)	Peak temp. in DSC (°C)	ΔH (kJ mol^{-1})
$VO(PTO)_2$	148–165	152	28.9	160	−214.6
	165–258	225	30.1	245	−63.7
	258–420	438	12.8	309, 327	−37.2
	420–450				Exo
$Cr(PTO)_3$	175–320	240	48.0	240	−218.4
	320–405	422	18.5		
	405–430				
	430–750	472	17.4	482	−3180
$Mn(PTO)_2 \cdot H_2O$	70–140	110	5.5	110	40.2
	240–320	260	51.4	256, 260	−348.7
	320–560	510	14.9	405, 475, 538	−50.0, −70.7, −3345
$Fe(PTO)_3$	180–248	196	76.5	205	−300.8
				272	−361.0
	335–470	375	6.6	372, 468	−1715, −80.9
$Co(PTO)_2$	215–240	225	41.5	227	−487.0
	240–470	345	12.1		
	470–505	502	19.3		
	505–550	533		553	−3881
$Ni(PTO)_2$				257	29.3
	255–305	283	18.4	283	−308.7
	305–480	446	12.2	442	−48.7
	480–610	521	46.6	549	−3551
$Cu(PTO)_2$	240–280	268	29.8	270, 277	−302.7
	280–395	320	10.0	340	−45.8
	395–610	494	33.7	477, 547	Exo
	660–900	750	9.4		
$Zn(PTO)_2$				260	43.5
	255–320	294	23.7	285	−177.9
	320–447	350	25.6		
	447–615	568, 590	20.1	578	Exo
	740–900	855	7.8		

with the elimination of a ligand molecule and a pyridine fragment (obs., 48.0%; calc., 47.5%). From 320 to 405 °C, a slow mass loss occurs. This is followed by a sudden decomposition which ends at 430 °C. The observed mass loss for both events is 18.5%, suggesting that a second pyridine fragment is eliminated (calc., 18.1%). Above 430 °C, a new weight loss takes place leaving Cr_2O_3 as the final product. This represents 16.1% of the initial mass of the complex (calc., 17.6%).

The DSC curve shows two exothermic peaks in the instrumental temperature range, at 240 and 482 °C, corresponding to the first and last steps in the DTG curve. The peak at 482 °C is very strong and seems to mask the effect due to the release of the second pyridine fragment.

$Mn(PTO)_2 \cdot H_2O$

The manganese(II) complex shows a mass loss between 70 and 140 °C, corresponding to the liberation of a water molecule (obs., 5.5%; calc., 5.7%). The expected endothermic behaviour of this process ($\Delta H = 40.2$ kJ mol^{-1}) appears in the DSC curve in the same temperature range. These values of temperature and enthalpy suggest that the water present is more like lattice water than coordinated water. The presence of two absorption peaks in the IR spectrum at 3370 and 1655 cm^{-1}, and the absence of bands due to the rocking, wagging or Mn–OH_2 stretching vibrations, is consistent with the above proposal [23]. Between 240 and 320 °C, a sudden 51.4% mass loss occurs. This can be assigned to the combined release of a pyridine *N*-oxide fragment and a pyridine fragment (calc., 52.9%). In this temperature range, the DSC curve displays two overlapping exothermic effects with maxima at 256 and 260 °C, parallel to the above effect. From 320 °C, a slow weight loss takes place which ends at 560 °C. This stage gives rise to the exothermic effects at 405, 475 and 538 °C. Beyond 560 °C, the weight stabilises. The residue at 740 °C is 28.2% of the initial sample. The X-ray diffraction pattern of this residue reveals the presence of Mn_2O_3 (calc., 24.3%) and $MnSO_4$ (calc., 46.4%), the former as major phase.

$Fe(PTO)_3$

The thermogravimetric analysis of the Fe(III) complex shows a mass loss between 180 and 248 °C. The observed weight loss (76.5%) is correlated with full decomposition of the complex and formation of Fe_2S_3 (theor., 76.1%). This effect is accompanied by a narrow exothermic peak at 205 °C. At 272 °C, another exothermic peak can be seen which, according to Schrader and Piltzsch [24], is due to the decomposition of Fe_2S_3 to FeS_2 and FeS. The oxidation of these compounds gives rise to the mass loss between 335 and 470 °C and the presence of the two exothermic events at 372 and 468 °C.

The final residue at 510 °C amounts to 16.9% of the original sample and is Fe_2O_3, as revealed by X-ray diffraction and IR-spectroscopy (calc., 18.4%).

Co(PTO)$_2$

As can be seen from the DTG curve, the first mass loss starts at 215 °C and finishes at 240 °C. The observed mass loss for this process (41.5%) compares favourably with the theoretical value corresponding to the elimination of a ligand molecule (40.5%). Beyond 240 °C and up to 470 °C, a slow decomposition takes place which is due to the expulsion of half a pyridine fragment (obs., 12.1%; calc., 12.6%). From 470 °C to the end of the run, a rapid weight loss occurs in two steps (470–505, and 505–550 °C). The percentage of the residue at 550 °C (27.1%) corresponds to Co_2O_3, confirmed by X-ray diffraction and IR spectroscopy (calc., 26.6%). The DSC curve shows a very narrow peak at 227 °C and a broad effect at 553 °C, both exothermic. Furthermore, an exothermic effect, without clear peaks, can be seen in the range of temperatures corresponding to the release of the pyridine derivative.

Ni(PTO)$_2$

The DSC curve of $Ni(PTO)_2$ shows a peak at 257 °C corresponding to fusion. The value of the fusion enthalpy calculated from the area of this peak is 29.3 kJ mol^{-1}. Liquid $Ni(PTO)_2$ decomposes immediately, indicated by an exothermic peak at 283 °C. This effect is accompanied by 18.4% weight loss below 305 °C, which could be correlated with the elimination of half a pyridine-2-thione molecule (calc. 17.7%). From 305 to 480 °C, a very slow mass loss occurs corresponding to the release of half a pyridine ring from the ligand (exp., 12.2%; calc., 12.6%). The DSC curve shows an exothermic peak at 442 °C which correlates with the above decomposition. Finally, from 480 °C, the weight continues to fall up to 610 °C, and then stabilises. The decomposition reaction is highly exothermic and exhibits a peak with a maximum at 549 °C. The weight of the final residue (22.8%), identified as NiO, is in good agreement with the calculated value (24.0%).

Cu(PTO)$_2$

The TG curve of $Cu(PTO)_2$ shows a first mass loss in the 240–280 °C range, which can be ascribed to the release of a pyridine *N*-oxide fragment (exp., 29.8%; calc., 29.8%). This effect overlaps with a second decomposition step between 280 and 395 °C, which corresponds to the elimination of a sulphur atom (exp., 10.0%; calc., 10.1%). A third mass loss occurs between 395 and 610 °C which leads to the formation of Cu_2OSO_4 and a little CuO, as revealed by the X-ray diffraction pattern (exp., 33.7%; calc. for Cu_2OSO_4,

37.9%, and for CuO, 25.2%). In the range 610–660 °C, the weight remains essentially unchanged. Above this, the desulphuration of the basic sulphate begins, giving rise to the formation of CuO. With temperature increase, CuO is slowly reduced to Cu_2O. A mixture of both oxides is detected in the crucible at 900 °C (exp., 24.3%; calc. for Cu_2O, 22.7%).

In the DSC curve, five exothermic peaks are observed below 600 °C. The double peak at 270 and 277 °C is attributed to the elimination of the pyridine *N*-oxide fragment. The peak at 340 °C corresponds to the release of the sulphur atom. Finally, the very strong effects at 477 and 547 °C can be correlated with the transformation to the mixture of Cu_2OSO_4 and CuO.

$Zn(PTO)_2$

For the $Zn(PTO)_2$ complex, the DSC trace shows a narrow endothermic peak at 260 °C which can be assigned to the melting of the solid. The enthalpy of fusion has a value of 43.5 kJ mol^{-1}. This is immediately followed by an exothermic peak at 285 °C, associated with a mass loss below 320 °C, which amounts to 23.7%. This value is in good agreement with the theoretical value required for the removal of a pyridine fragment (24.6%). Between 320 and 447 °C, a further pyridine fragment is released (obs. mass loss, 25.6%). The thermal degradation of the sample continues up to 615 °C, giving a residue of ZnS (obs., 30.6%; calc., 30.7%). A broad exothermic peak, with maximum at 578 °C, correlates with the above weight loss. This effect probably masks the thermal behaviour corresponding to the liberation of the second pyridine fragment. In the range 615–740 °C, the mass remains essentially unchanged. Then ZnS breaks down to give ZnO as the only product. It should be stressed that the observed weight at 900 °C is smaller than that calculated from the empirical formula (exp., 22.8%; theor., 25.6%). This can be attributed to a partial sublimation of zinc sulphide, simultaneous with the oxidation process [25].

Order stability

In accordance with the value of the initial temperature of the first exothermic decomposition and the value of the peak in the DSC curve, the order of thermal stability of the complexes is VO(IV) < Fe(III) < Co(II) < Cr(III) < Mn(II) < Cu(II) < Ni(II) ≤ Zn(II). This order seems to be determined by the structure of the compounds: Fe(III) and Cr(III) complexes have octahedral geometry [2]; Co(II) and VO(IV) complexes show the same structure by oligomerisation [3,26]; the Mn(II) compound is tetrahedral; the Cu(II) and Ni(II) complexes are square-planar; and the Zn(II) complex has a trigonal bipyramidal geometry [5].

REFERENCES

1 R.A. Jones and A.R. Katritzky, J. Chem. Soc., (1960) 2937.
2 M.A. Robinson, J. Inorg. Nucl. Chem., 26 (1964) 1227.
3 A. Hodge, K. Nordquest and E.L. Blinn, Inorg. Chim. Acta, 6 (1972) 491.
4 H.J. Friese and F. Umland, Fresenius' Z. Anal. Chem., 287 (1977) 298.
5 B.L. Barnett and H.C. Kretschmar, Inorg. Chem., 16 (1977) 1834.
6 D.X. West and C.A. Frank, J. Inorg. Nucl. Chem., 41 (1979) 49.
7 D.R. Brown and D.X. West, J. Inorg. Nucl. Chem., 43 (1981) 1017.
8 J.L. Davidson, P.N. Preston and M.V. Russo, J. Chem. Soc., Dalton Trans., (1983) 783.
9 M.C.R. Simons and D.X. West, J. Chem. Soc., Dalton Trans., (1985) 379.
10 F.E. Pansy, H. Stander, W.L. Koerber and R. Donovick, Biol. Med., 82 (1953) 122.
11 J.A. Box, D.S. Shanga, N. Sanghvi and J.K. Sugden, Pharm. Acta Helv., 55 (1980) 120.
12 K.J. McGinley and J.J. Leyden, Arch. Dermatol. Res., 272 (1982) 339.
13 C.J. Chandler and I.H. Segel, Antimicrob. Agents Chemother., 14 (1978) 60.
14 J.D. Nelson and G.A. Hyde, Cosmet. Toiletries, 96 (1981) 87.
15 E.O. Bennett, J.E. Gannon and I.U. Onyekweln, Int. Biodeterior, Bull., 18 (1982) 7.
16 J.A.W. Dalziel and M. Thompson, Analyst, 89 (1964) 707.
17 M. Edrissi, A. Massoumi and J.A.W. Dalziel, Microchem. J., 15 (1970) 579.
18 M. Edrissi, A. Massoumi and M. de la Rezaza, Anal. Chim. Acta, 71 (1974) 215.
19 M. Edrissi, M.J. Jadeabe and J.A.W. Dalziel, Microchem. J., 16 (1971) 526.
20 M. Edrissi and A. Massoumi, Microchem. J., 16 (1971) 177.
21 M. Edrissi, A. Massoumi and J.A.W. Dalziel, Microchem. J., 16 (1971) 538.
22 G. Charlot, Colorimetric Determination of Elements, Elsevier, Amsterdam, 1964.
23 K. Nakamoto, Infrared and Raman Spectra of Inorganic and Coordination Compounds, 3rd edn., Wiley, New York, 1978, p. 227.
24 R. Schrader and C. Piltzsch, Krist. Tech., 4 (1969) 385.
25 R. Dimitrov and I. Bonev, Thermochim. Acta, 106 (1986) 9.
26 A. Pérez-Florindo, Doctoral Thesis, Universidad de Extremadura, Badajoz, 1988.